Highly sensitive and broadband carbon nanotube radio-frequency single-electron transistor

S. E. S. Andresen,[1] F. Wu,[2] R. Danneau,[2] D. Gunnarsson,[2] and P. J. Hakonen [2,*]

[1] *Niels Bohr Institute, Nano-Science Center, University of Copenhagen,*
Universitetsparken 5, DK-2100 København Ø, Denmark
[2] *Low Temperature Laboratory, Helsinki University of Technology,*
P.O. BOX 2200, FIN-02015 HUT, Finland

We have investigated radio-frequency single-electron transistor operation of single-walled carbon nanotube quantum dots in the strong tunneling regime. At a temperature of 4.2 K and with carrier frequency 754.2 MHz, we reach a charge sensitivity of $2.3 \times 10^{-6} \, e/\sqrt{\text{Hz}}$ over a bandwidth of 85 MHz. Our results indicate a gain-bandwidth product of 3.7×10^{13} $\text{Hz}^{3/2}/e$, which is by one order of magnitude better than for typical RF-SETs.

I. INTRODUCTION

The single-electron transistor (SET) is a highly sensitive electrometer, conventionally based on sequential tunneling of electrons in the Coulomb blockade regime.[1] Unfortunately, the RC-time due to cable capacitance ($C \sim 1$ nF) and device resistance ($R \sim 100\text{k}\Omega$) limits the bandwidth to a few kHz. This is a major drawback for the direct application of SETs as it limits the operation to a regime where $1/f$-noise is strong, either due to background charge noise,[2] or to variations in the tunneling resistance.[3]

The limitation on the frequency bandwidth can be bypassed using microwave techniques for reading out the real part of the SET impedance. In these so called RF-SETs,[4] an LC-circuit is used to transform the high impedance of the SET to a high-frequency setup with a characteristic impedance of $Z_0 = 50 \, \Omega$. The transformation is frequency selective, and a good match is obtained only over a frequency range $f_0 \pm f_0/Q$, where $f_0 = 1/(2\pi\sqrt{LC})$ is the resonant frequency of the matching circuit, and $Q = \sqrt{L/C}/Z_0$ under fully matched conditions. Typical charge sensitivities of RF-SETs amount to $10^{-5} \, e/\sqrt{\text{Hz}}$ over a signal bandwidth of 20 MHz.[4]

In order to improve the performance of RF-SETs, the operating regime has to be brought from sequential tunneling to co-tunneling, i.e., from the weak to the strong tunneling regime.[5] The energy sensitivity including back action noise has been estimated to be $\sim 2\hbar$ in the sequential tunneling regime.[6] In the co-tunneling regime, the sensitivity is expected to approach $0.5\hbar$.[5] Another benefit of the strong tunneling regime is that a wider bandwidth can be obtained as the Q-factor can be made smaller. However, the effective Coulomb energy diminishes rapidly with lowering resistance R_T of the tunnel barriers. This behavior has been summarized for single junctions by Wang et al.[7] They find, e.g., that $E_C^{\text{eff}} = 0.3E_C$ for $R_T = 3$ kΩ. Provided that $E_C^{\text{eff}} \gg k_B T$, the strong tun-

neling SETs are expected to operate well as RF-SETs.[8] This regime of operation has been strived for by Brenning et al.[9] They managed to fabricate Al/AlO$_x$ tunnel junction SETs with $E_C/k_B = 18$ K, and a total resistance of $R_\Sigma = 25$ kΩ. For the charge sensitivity, they reached $\delta q = 1.9 \times 10^{-6} \, e/\sqrt{\text{Hz}}$ at 4.2 K, which is the best liquid helium result obtained so far.

Single-walled carbon nanotubes (SWCNTs) provide an alternative approach to the metallic SETs in the strong tunneling regime. The first reports on single-electron charging effects in individual tubes and bundles were published in 1997.[10,11] Charging energies of about 30 meV were quickly observed.[12] Since then, contacting techniques have greatly improved, and impedances of 10–20 kΩ can be rather routinely obtained, e.g., using Pd contacts.[13] SWCNTs with large E_C are very promising for RF-SETs, especially since their shot noise has been found to be well below the Schottky value.[14]

In this article, we report on RF-SETs made from SWCNTs in the strong tunneling regime. We find a charge sensitivity of $\delta q = 2.3 \times 10^{-6} \, e/\sqrt{\text{Hz}}$ at 4.2 K, which nearly equals that obtained by Brenning et al.[9] Compared with previous carbon nanotube RF-SETs,[15,16,17] the improvement is by a factor ranging from 7 to 200. In combination with a bandwidth of 85 MHz, our results represent a considerable improvement for broadband charge sensing, e.g., for fast read-out of single-electron devices such as quantum dots.

II. DEVICE FABRICATION AND EXPERIMENTAL SETUP

Our SWCNTs are grown from patterned catalyst islands, following the approach of Kong et al.[18,19] RF-SET operation necessitates the use of insulating substrates in order to minimize the shunt capacitance. We use sapphire for lower losses and charge noise compared to conventional Si/SiO$_2$. The chemical vapor deposition (CVD) takes place in a ceramic tube furnace from a gas mixture of Ar, H$_2$, and CH$_4$ at ~ 900 °C. After growth, pairs of 25/15 nm Ti/Au contacts, $0.3 \, \mu$m apart, are defined between the catalyst islands by electron beam lithography. A central top-gate, $0.1 \, \mu$m wide, is de-
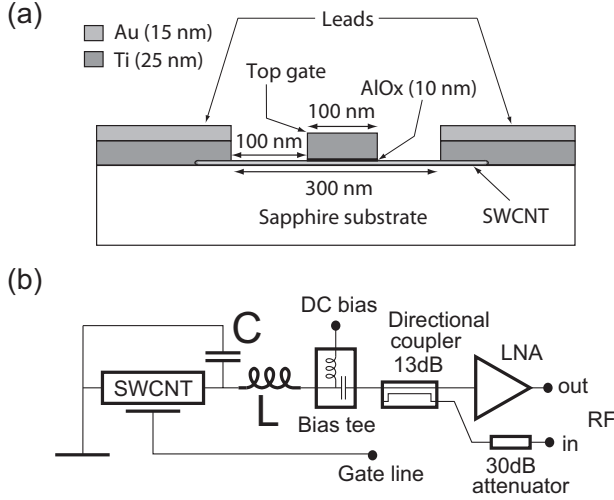
FIG. 1 (a) Layout side-view of the biasing leads and gate electrode connected to the single-walled carbon nanotube. (b) Experimental setup for RF-SET measurements, all immersed in liquid helium for cooling to 4.2 K.
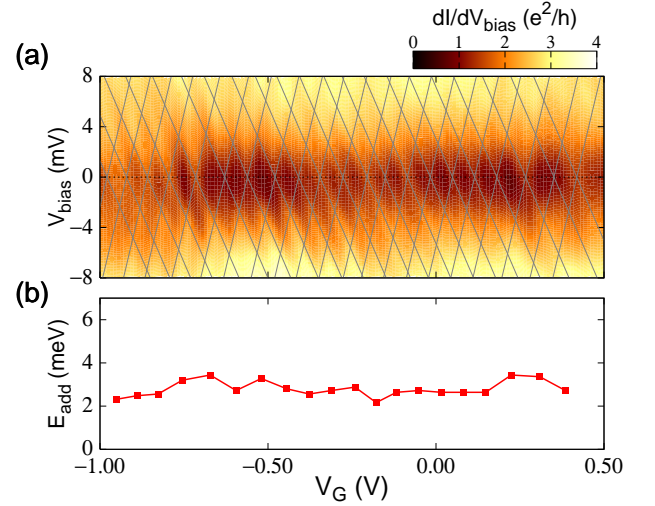

FIG. 2 (a) 2D-map of the differential conductance dI/dV_{bias} in units of e^2/h as a function of gate voltage V_G and bias voltage V_{bias}. The lines mark the charge degeneracies. (b) Values of the addition energy E_{add} deduced from (a) as the degeneracy crossings in V_{bias}.

posited between the contacts. Under the actual 25 nm Ti gate, an insulating barrier is formed by five 2 nm Al layers, each oxidized 2 min at atmosphere. Finally, we deposit a Cr/Au mask with 230 μm bond-pads. The final device layout is illustrated in Fig. 1(a).

A schematic of the low-temperature measurement setup is shown in Fig. 1(b).[21] The sample connects to an LC-circuit, formed by the inductance $L = 150$ nH of a surface mount inductor and the bond-wires, and the parasitic capacitance $C = 0.3$ pF of the bond-pads. The circuit is connected to a coplanar transmission line with a surface mount bias-tee that couples the DC-bias and RF-signal. The top-gate is connected to a separate coaxial line for high-bandwidth modulation. We use a home-made low-noise amplifier with a frequency range of 600–950 MHz.[20] The RF-input is coupled to the coaxial line through a 13 dB directional coupler and a 30 dB attenuator that reduces the noise from room temperature. The RF-output is detected in a fashion dependent of the goal of the measurement: 1) by a spectrum analyzer to investigate the carrier modulation spectra, or 2) by mixer demodulation for homodyne detection at a particular frequency.

III. RESULTS AND DISCUSSION

Fig. 2(a) shows the differential conductance (dI/dV_{bias}) versus gate and bias voltages (V_G, V_{bias}). For $V_{bias} > 6$ mV, $dI/dV_{bias} = 3.0$–3.5 e^2/h, indicating a high-quality SWCNT sample with highly transparent contacts. However, there is a clear but smooth Coulomb modulation pattern at $V_{bias} = 0$. As such, the sample behaves as a SET in the strong tunneling regime. By tracing the Coulomb diamonds, we find the addition energies $E_{add} = 2E_C + \Delta E_N$, with Coulomb energy $E_C = e^2/(2C_\Sigma)$ and level spacing $\Delta E_N = E_N - E_{N-1}$. The

values in Fig. 2(b) cover the range 2.2–3.4 meV, which sets an upper bound of $E_C/k_B = 12.8$ K, corresponding to a total capacitance of the SET island of $C_\Sigma \sim 73$ aF. From the gate modulation and slopes of the diamonds in Fig. 2(a), we estimate that the gate capacitance $C_g \sim 2.9$ aF.

For RF-SET operation, the optimum operating point was found by searching for points of perfect matching, i.e., vanishing reflection at the resonance frequency $f_0 = 754.2$ MHz. The signal was homodyne detected by mixer, and the phase was tuned to be sensitive only to the real part of the SET impedance. We found three points around $V_G = 0.63$–0.72 V with maximum differential response, coinciding with perfect matching (Fig. 3(a)). Using a spectrum analyzer, the input carrier power was tuned to obtain maximum signal-to-noise ratio of the sidebands at $f_0 \pm f_{mod}$, while keeping a small gate-charge modulation of $q_{RMS} = 0.006e$ at $f_{mod} = 10$ MHz (Fig. 3(b)). The signal-to-noise ratio (SNR) of both sidebands yields a charge sensitivity of $\delta q = 2.3 \times 10^{-6}$ $e/\sqrt{Hz}$, corresponding to an uncoupled energy sensitivity of $\varepsilon = \delta q^2/(2C_\Sigma) \sim 9\hbar$. The frequency response was mapped out by repeating the sensitivity measurement over a range of modulation frequencies of 0.5–150 MHz (Fig. 3(c)). We found a bandwidth of 85 MHz and observed that $1/f$-noise only contributes significantly below 1–2 MHz.

Optimization of RF-SET sensitivity has been treated in several papers.[22,23,24,25] The ultimate shot noise limited sensitivity was found in Ref. 21 to be

$$\delta q = 2.65e\sqrt{R_\Sigma C_\Sigma \frac{k_B T}{e^2/C_\Sigma}}, \qquad (1)$$

which in our case ($R_\Sigma = 10$ kΩ, $C_\Sigma = 73$ aF) amounts to 0.9×10^{-6} $e/\sqrt{Hz}$. When the noise of the amplifier dominates the performance, the sensitivity scales with the noise amplitude
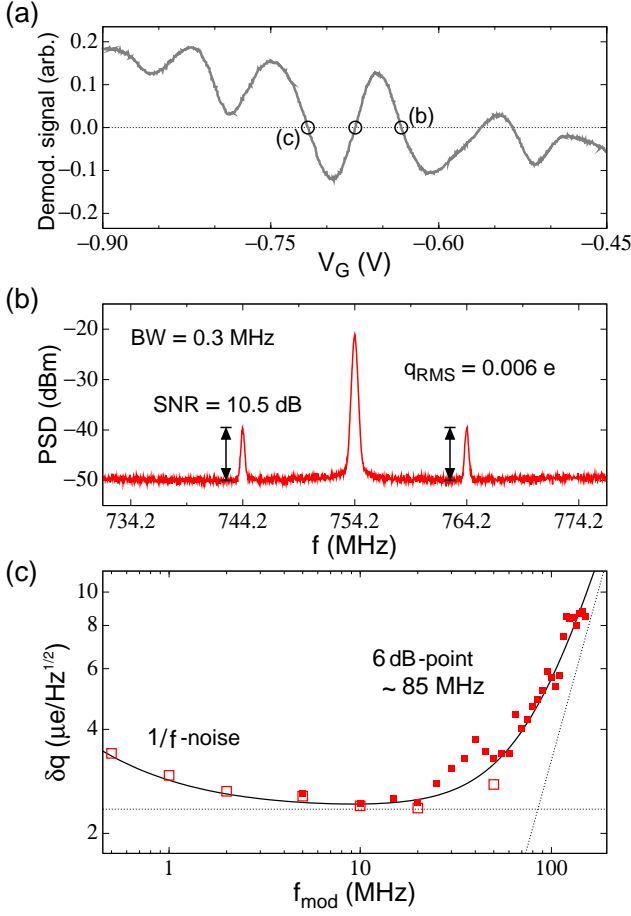
FIG. 3 (a) Demodulated signal averaged over 5000 gate voltage sweeps of each 2 μs. Circles mark the points of perfect matching used in (b) and (c). (b) Power spectrum (0.3 MHz spectral resolution) under 754.2 MHz carrier excitation (-65 dBm) and 10 MHz gate modulation of $0.006\,e$. (c) Charge sensitivity versus modulation frequency f_{mod}, with/without a 100 MHz low-pass filter on the gate-line (open/filled symbols). The lines indicate the roll-off limited by the bandwidth and $1/f$-noise at low frequency.

and the differential response of the RF reflectance ($\partial\Gamma/\partial q$) as

$$\delta q = \frac{\sqrt{2\,k_{\mathrm{B}}T_{\mathrm{N}}Z_0}}{v_0 \times |\partial\Gamma/\partial q|}, \tag{2}$$

where T_{N} denotes the noise temperature of the amplifier and v_0 the amplitude of the RF carrier signal. In our case, the amplitude over the SET is $v_{\mathrm{S}} = v_0\sqrt{R_\Sigma/Z_0} \sim 2$ mV at perfect matching. In Ref. 23, an approximation of Eq. (2) was found from the orthodox theory as

$$\frac{\delta q}{e} = 1.46 \times 10^{-6} \times \left(\frac{k_{\mathrm{B}}T}{E_{\mathrm{C}}}\right)^{0.59} E_{\mathrm{C}}(\mathrm{K})^{-1.01}$$
$$\times \left(\frac{R_\Sigma}{Z_{\mathrm{T}}}\right)^{0.91} T_{\mathrm{N}}(\mathrm{K})^{0.5}, \tag{3}$$

with E_{C} and T_{N} in units of K, and $Z_{\mathrm{T}} = \sqrt{L/C}$. Assuming that heating does not play a significant role, we estimate from

Eq. (3) that $\delta q = 1.3 \times 10^{-6}\,e/\sqrt{\mathrm{Hz}}$, taking $E_{\mathrm{C}}/k_{\mathrm{B}} = 12.8$ K, $R_\Sigma = 10$ kΩ, $Z_{\mathrm{T}} = 0.71$ kΩ, and $T_{\mathrm{N}} = 4.2$ K. All of these estimates are based on the classical orthodox theory for Coulomb blockade,[1] which is only valid in the weak tunneling regime. However, as discussed above, we are in the strong tunneling regime. One way around this issue is simply to adopt the effective charging energy $E_{\mathrm{C}}^{\mathrm{eff}} = 0.75 E_{\mathrm{C}}$, calculated by Wang et al.[7] Then the estimate for the charge sensitivity becomes $\delta q = 2.1 \times 10^{-6}\,e/\sqrt{\mathrm{Hz}}$, which agrees well with the measured value. In making our estimates, we have neglected the effects of quantum level spacing (see discussion in Ref. 30).

IV. CONCLUSIONS

We have shown that a SWCNT quantum dot in the strong tunneling regime can be operated as an excellent RF-SET at liquid helium temperature (4.2 K). We obtain a charge sensitivity of $\delta q = 2.3 \times 10^{-6}\,e/\sqrt{\mathrm{Hz}}$, which is nearly as good as the best Al/AlO$_x$ results.[9] It represents an enhancement of at least a factor of 7 compared with previous carbon nanotube RF-SETs.[15,16,17] Very recently, comparable sensitivities were achieved with other types of SETs: 1) InAs/InP heterostructured nanowires,[26] and 2) electrostatically defined Si quantum dots.[27]

With a bandwidth of 85 MHz, our gain-bandwidth product amounts to 3.7×10^{13} Hz$^{3/2}/e$, where gain is defined as $1/\delta q$. That is by more than one order of magnitude better than for typical RF-SETs.[4] Therefore, SWCNT based RF-SETs may have value in applications where high speed is needed. One possible application is for charge sensing on quantum dots in the context of quantum computing. Here, the coupling to a nearby quantum dot structure, e.g., another nanotube, could be achieved via an antenna gate as it was recently demonstrated with SiGe nanowires.[28]

The best way to enhance the sensitivity further would be to lower the temperature so the Coulomb modulation is fully developed. For Al/AlO$_x$ junction SETs, the improvement at 40 mK was $\delta q = 0.9\,e/\sqrt{\mathrm{Hz}}$ in the superconducting state and $\delta q = 1.0\,e/\sqrt{\mathrm{Hz}}$ in the normal state.[9] To improve the bandwidth, the only option is to increase the resonance frequency of the LC-circuit. The limit set by the Bode-Fano criterium states that the maximum achievable bandwidth is $(2R_\Sigma C)^{-1}$, which in our case amounts to ~ 170 MHz.

References

[1] See, e.g., K. K. Likharev, Proc. IEEE **87**, 606 (1999).

[2] B. Starmark, T. Henning, T. Claeson, P. Delsing, and A. N. Korotkov, J. Appl. Phys. **86**, 2132 (1999).

[3] V. Krupenin, D. Presnov, M. Savvateev, H. Scherer, A. Zorin, and J. Niemeyer, J. Appl. Phys. **84**, 3212 (1998).

[4] R. J. Schoelkopf, P. Wahlgren, A. A. Kozhevnikov, P. Delsing, and D. E. Prober, Science **280**, 1238 (1998).

[5] D. Averin, in *Macroscopic Quantum Coherence and Quantum Computing*, edited by D. V. Averin, B. Ruggiero, and P. Silvestrini (Kluwer, New York, 2001) pp. 399–408; arXiv:cond-mat/0010052.

[6] M. H. Devoret, R. J. Schoelkopf, Nature **406**, 1039 (2000)

[7] X. Wang, R. Egger and H. Grabert, Europhys. Lett. **38**, 545 (1997).

[8] P. Wahlgren, Ph.D. thesis, Chalmers University of Technology, unpublished (1998).

[9] H. Brenning, S. Kafanov, T. Duty, S. Kubatkin and P. Delsing, J. Appl. Phys. **100**, 114321 (2006).

[10] S. J. Tans, M. H. Devoret, H. Dai, A. Thess, R. S. Smalley, L. J. Geerlings, and C. Dekker, Nature (London) **386**, 474 (1997).

[11] M. Bockrath, D. H. Cobden, P. L. McEuen, N. G. Chopra, A. Zettl, A. Thess, and R. E. Smalley, Science **275**, 1922 (1997).

[12] J. Nygard, D. H. Cobden, M. Bockrath, P. L. McEuen, and P. E. Lindelof, Applied Physics A **69**, 297 (1999).

[13] A. Javey, J. Guo, Q. Wang, M. Lundstrom, and H. Dai, Nature **424**, 654 (2003).

[14] F. Wu, P. Queipo, A. Nasibulin, T. Tsuneta, T. H. Wang, E. Kauppinen and P. J. Hakonen, Phys. Rev. Lett. **99**, 156803 (2007).

[15] L. Roschier, M. Sillanpää, W. Taihong, M. Ahlskog, S. Iijima, and P. Hakonen, J. Low Temperature Phys. **136**, 465 (2004).

[16] M. J. Biercuk, D. J. Reilly, T. M. Buehler, V. C. Chan, J. M. Chow, R. G. Clark, and C. M. Marcus, Phys. Rev. B **73**, 201402 (2006).

[17] Y. Tang, I. Amlani, A. O. Orlov, G. L. Snider, and P. J. Fay, Nanotech. **18**, 445203 (2007).

[18] J. Kong, H. T. Soh, A. M. Cassell, C. F. Quate, and H. Dai, Nature **395**, 878 (1998).

[19] K. Grove-Rasmussen, H. I. Jørgensen, and P. E. Lindelof, Proceeding Int. Symp. on Mesoscopic Superconductivity and Spintronics 2006, NTT BRL, Atsugi, Japan, World Scientific Publishing (2007).

[20] L. Roschier and P. Hakonen, Cryogenics **44**, 783 (2004).

[21] F. Wu, L. Roschier, T. Tsuneta, M. Paalanen, T. H. Wang, and P. Hakonen, AIP Proc. **850**, 1482 (2006).

[22] A. N. Korotkov and M. A. Paalanen, Appl. Phys. Lett. **74**, 4052 (1999).

[23] L. Roschier, P. Hakonen, K. Bladh, P. Delsing, K. W. Lehnert, L. Spietz, and R. J. Schoelkopf, J. Appl. Phys. **95**, 1274 (2004).

[24] V. O. Turin and A. N. Korotkov, App. Phys. Lett. **83**, 2898 (2003).

[25] V. O. Turin and A. N. Korotkov, Phys. Rev. B **69**, 195310 (2004).

[26] H. A. Nilsson, T. Duty, S. Abay, C. Wilson, J. B. Wagner, C. Thelander, P. Delsing, and L. Samuelson, Nano Lett. **8**, 872 (2008).

[27] S. J. Angus, A. J. Ferguson, A. S. Dzurak, and R. G. Clark, Appl. Phys. Lett. **92**, 112103 (2008).

[28] Y. Hu, H. O. H. Churchill, D. J. Reilly, J. Xiang, C. M. Lieber, and C. M. Marcus, Nature Nanotech. **2**, 622 (2007).

[29] C. W. J. Beenakker, Phys . Rev. B **44**, 1646 (1991).

[30] By studying the Coulomb diamond pattern around the optimum sensitivity we deduce that $E_C \sim \Delta E_N$ and $\Delta E_N \sim 3k_B T$. This suggests that we are in the quantum Coulomb blockade regime (QCB), where $k_B T \ll \Delta E_N < 2E_C$ and only few levels are involved in transport. However, comparing the conductance peak line-shapes around optimum sensitivity with theory[29], we find deviations between the experimental data and QCB predictions. From the experimental data we get $G_N = G/G_\infty \sim 0.45$ at peak maximum and $dG_N/dV_G \sim 10$ V^{-1} as optimum transconductance. These values should be compared to $G_N \sim 0.75$ and $dG_N/dV_G \sim 40$ V^{-1} as predicted by theory. Also the predictions from the metallic Coulomb blockade regime with $G_N \sim 0.5$ and $dG_N/dV_G \sim 20$ V^{-1} are deviating, but the peak maximum is close to the measured. This discrepancy is explained by the fact that we are in the strong tunneling regime with $R_Q/R_\Sigma \sim 2.5$ which broadens the energy levels. Since we still have strong Coulomb blockade we are not quite in the Breit-Wigner limit, but rather in an intermediate regime $k_B T < h\Gamma \sim \Delta E_N < 2E_C$ which behaves closest to the strong tunneling description.